Available online at www.sciencedirect.com

ScienceDirect

journal homepage: http://www.elsevier.com/locate/acme

Original Research Article

Modeling of cutter displacements during ball end milling of inclined surfaces

S. Wojciechowski [a,*], T. Chwalczuk [a], P. Twardowski [a], G.M. Krolczyk [b]

[a] Poznan University of Technology, Piotrowo 3, Poznan 60-965, Poland
[b] Opole University of Technology, Proszkowska 76, Opole 45-758, Poland

ARTICLE INFO

Article history:
Received 19 February 2015
Accepted 28 June 2015
Available online 1 August 2015

Keywords:
Ball end milling
Dynamics
Run out

ABSTRACT

This work concentrates on the modeling of cutter's displacements during ball end milling with various surface inclinations. The cutter's displacements (vibrations) model including: tool's geometry, cutting conditions, surface inclination angle, run out and tool's deflections (induced by the cutting forces) was proposed. Subsequently, this model was validated empirically during the milling tests with various feed per tooth (f_z), depth of cut (a_p) and surface inclination angle (α) values. Experiments were carried out with the application of laser displacement sensor and force dynamometer. The research revealed that cutter's displacements are strongly affected by the cutter's run out and surface inclination. This observation is also confirmed by the developed model.

1. Introduction

Ball end milling process of the curvilinear surfaces is very often conducted in the finishing conditions, that is, with axial depth of cut, a_p, lower than 0.3 mm and radial depth of cut, a_e, lower than 0.5 mm. For the above-mentioned applications manufacturing tolerances are very narrow, usually within the range 0.05–0.1 mm for stamping dies and less than 0.04 mm for injection molds made of hardened steels [1]. However, the measured form errors in the machined curvilinear surfaces very often exceed 100 μm [2]. Thus, the problem of the quality improvement in the complex surfaces needs extensive studies.

Many of researches related to the machined surface's texture focuses primarily on the influence of the cutting parameters [3]. Nevertheless, the machined surface's quality can be also affected by the other phenomena occurring during cutting, e.g. tool wear [4], burr formation at the edges of the work material [5], machined surface temperature [6] or process stability [7]. Another important source of the problems related to the surface's texture formation is cutter's displacement (vibrations). These displacements are mainly caused by the cutting and centrifugal forces, which induce tool's deflections, but also by the geometrical errors of the spindle–toolholder–milling tool system (e.g. static run out).

The numerous of works are focused on estimation of the tool's displacements on the basis of models which assume solely deflections induced by the cutting forces. As an example, Budak [8] estimated end mill's deflections on the basis of the cantilever and segmented beam models. Subsequently, this model was applied to the estimation of form errors during the peripheral milling of a plate made out of titanium Ti6Al4. Similar approaches were also adopted by Kim

* *Corresponding author*. Tel.: +48 061 6652608; fax: +48 061 6652200.
E-mail address: sjwojciechowski@o2.pl (S. Wojciechowski).
http://dx.doi.org/10.1016/j.acme.2015.06.008
1644-9665/

et al. [2] and López de Lacalle et al. [9], which were concentrated on the estimation of form and dimensional errors during the ball end milling of KP4M material in semi-finishing conditions and high speed ball end milling of hardened SKD 61 steels. The research results presented in the both works have revealed that errors obtained in the machined surfaces are affected by the machining strategies and surface inclination angles.

Nevertheless, deflection model based on a cantilever beam is not very accurate, but it can be useful to have an aim on the dimensional error's values in machining of complex surfaces. The moderate accuracy of this model can be attributed to the consideration of static deflections, instead of dynamical ones, which in turn are related to the modal parameters of the spindle–tool system and variable force signals. Therefore, the second model is based on the dynamical deflections, which are calculated on the basis of differential motion equation. As an example, Insperger et al. [10] estimated tool's deflections with the application of the standard 2 degrees of freedom oscillator. The model was applied to the assessment of the surface location errors (SLE) during the end milling of AlMgSi alloy in the semi-finishing conditions. The similar approach was presented by Twardowski et al. [11] to the estimation of surface roughness during high speed end milling of hardened X155CrVMo12-1 steel. Furthermore, the differential motion equation model was also applied to the estimation of the work piece's deflection during low radial immersion milling [12] and the surface roughness estimation of the thin wall milling [13]. With reference to the ball end mills, the dynamical deflection model was employed to the estimation of tool tip displacement during semi-finishing of sculptured surface made of CK45 carbon steel [14] and simulation of stability lobe for a ball end milling of titanium Ti6Al4V [15]. Nonetheless, the comparison of the modeled and measured tool's displacements was not presented in these works.

The dynamical deflection model is valid mainly for the machining processes with relatively large cross sectional area of cut values (e.g. roughing, semi-roughing), or/and for the machining with the slender tools. However, during finishing processes or machining with the application of the rigid tools, the geometrical errors of the spindle–toolholder–milling tool system have also the significant meaning. According to Sun and Guo [16] the static run out can significantly affect cutter's sweep surface during five-axis flank milling, and thus machined surface's quality. Additionally, the previous researches [17,18], related to the finishing end milling of the hardened 55NiCrMoV6 steel have revealed that milling tool's working part displacements measured by the laser vibrometer were affected both by the deflections induced by cutting forces and cutter's static radial run out.

From the literature survey presented above, it can be seen that problem of ball end mill displacements' estimation during machining is investigated unsatisfactorily, and thus needs further studies. The researches should focus on model's formulation, which includes the effect of cutter's deflection and run out phenomenon simultaneously, as well as the variation of surface inclination during milling of curvilinear surfaces. Furthermore, the reliable comparison of the modeled and measured tool's displacements should be also presented. Consequently, in this paper, the ball end mill's displacements model is proposed. This approach includes both deflections induced by the dynamical cutting forces and cutter's static radial run out, and thus it can be applied for the diversified milling operations, e.g. finishing or roughing. Subsequently, the developed model will be validated empirically with the application of laser displacement sensor, during the milling tests with various feed per tooth, axial depth of cut and surface inclination angle values.

2. Ball end mill's displacement model

The work presented in this paper focuses on the modeling and measurements of the ball end mill's instantaneous displacement $y(t)$, in the direction perpendicular to the tool's rotational axis and collinear to the feed motion vector (Fig. 1). In accordance to the previous researches [1,19], this direction has direct influence on the cutter's displacement y_e, which is perpendicular to the machined surface, and thus affects the surface texture formation (e.g. surface roughness or surface location errors). In this study, the end milling tool's working part displacements model, described in [18] is adopted. This model assumes that cutter's instantaneous displacements are caused by the geometrical errors of the spindle–toolholder–milling tool system y_r and tool's deflections y_d, induced by the variable cutting forces (Fig. 2).

The total tool's instantaneous displacement can be expressed by the following equation:

$$y(t) = y_r(t) + y_d(t) \tag{1}$$

The value of tool's displacement y_r is usually related to the static radial run out e_r, which can be induced by the tool itself (wear, asymmetry, insert setting, dynamic imbalance and thermal deformation) or the offset between the position of tool's rotation axis and spindle's rotation axis. The consequence is a tool rotation around the spindle axis with an eccentricity, which induces cutter displacements.

The instantaneous displacement y_r for the ball end mill, related to the static radial run out e_r can be calculated from the expression:

$$y_r(t) = -(e_r) \cdot \sin\left(\frac{\pi \cdot n \cdot t}{30} - \frac{\psi_{l1} + \psi_{l2}}{2} + \delta\right) \tag{2}$$

where: ψ_{l1}, ψ_{l2} are the initial and final lag angles [rad], δ is the radial run out's angle [rad], e_r is the static radial run out

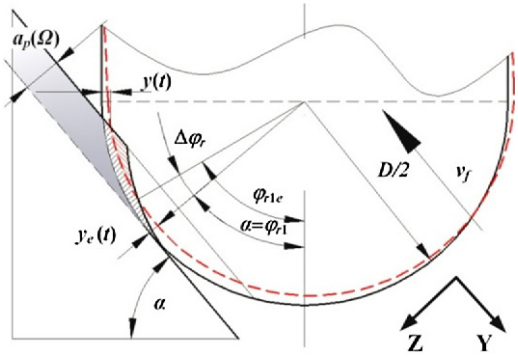

Fig. 1 – Instantaneous cutter's displacements: $y(t)$ and $y_e(t)$ during ball end milling with surface inclination ($\alpha > 0$).

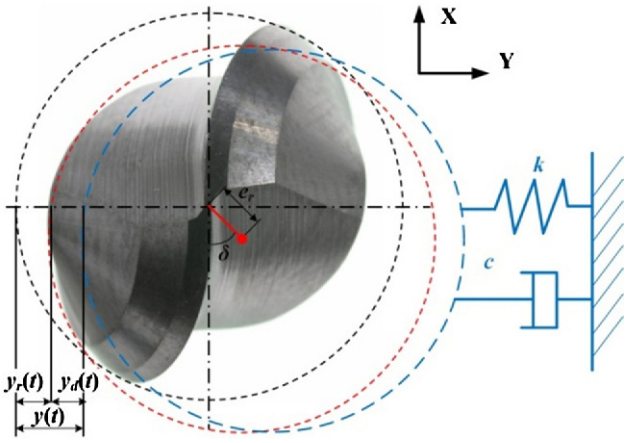

Fig. 2 – The model of instantaneous cutter's displacement y(t) for the ball end mill.

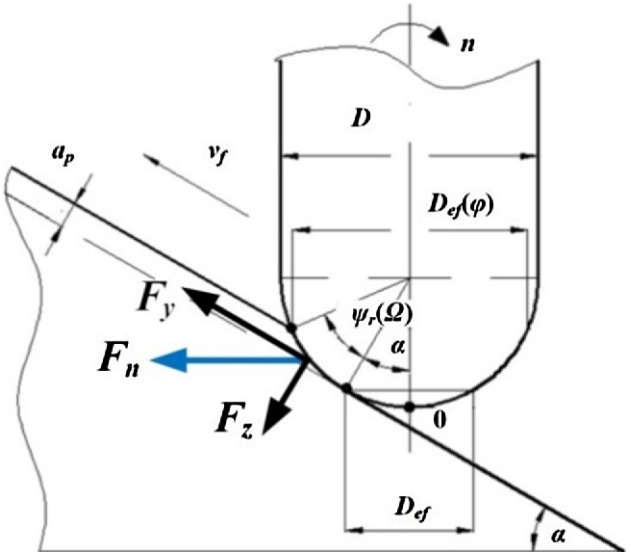

Fig. 3 – The designation of the normal force $F_n(t)$ during ball end milling of inclined surface.

[μm], n is the spindle rotational speed [rev/min], t is the time [s].

The instantaneous deflections $y_d(t)$ of the ball end mill, induced by cutting forces can be calculated on the basis of the differential motion equation:

$$m \cdot \ddot{y}_d(t) + c \cdot \dot{y}_d(t) + k \cdot y_d(t) = F_n(t) \tag{3}$$

where: m, c, k are the modal parameters, namely: mass [Ns^2/m], damping coefficient [N s/m], stiffness coefficient [N/m], $F_n(t)$ is the instantaneous normal force [N].

Eq. (3) was solved numerically in MATLAB Simulink software with the application of a variable step Runge–Kutta method (ode45 solver).

The instantaneous normal force $F_n(t)$, included in Eq. (3) is perpendicular to the tool's rotational axis and collinear to the feed motion vector. According to Fig. 3, its value is depended on cutting forces in machine tool's coordinate system (F_y, F_z) and surface inclination angle α. This dependency is described by the following equation:

$$F_n(t) = F_z(t) \cdot \sin\alpha + F_y(t) \cdot \cos\alpha \tag{4}$$

Eq. (4) and Fig. 3 reveal that in case of ball end milling with low surface inclinations, cutter's deflections are caused mainly by cutting forces in feed direction (F_y), whereas during the milling with high surface inclinations, they are induced primarily by the thrust force (F_z). The instantaneous values of F_y and F_z forces, can be calculated on the basis of the mechanistic approach, described by equations:

$$F_y(t) = \sum_{j=1}^{z_c}[-(K_{re}l_j + K_{rc}A_{zj}) \cdot \sin\varphi_{rj}\sin\varphi_j - (K_{ae}l_j + K_{ac}A_{zj}) \cdot \cos\varphi_{rj} \cdot \sin\varphi_j - (K_{te}l_j + K_{tc}A_{zj}) \cdot \cos\varphi_j] \tag{5}$$

$$F_z(t) = \sum_{j=1}^{z_c}[(K_{re}l_j + K_{rc}A_{zj}) \cdot \cos\varphi_{rj} - (K_{ae}l_j + K_{ac}A_{zj}) \cdot \sin\varphi_{rj}] \tag{6}$$

where: K_{te}, K_{re}, K_{ae} are the edge specific coefficients [N/mm], K_{tc}, K_{rc}, K_{ac} are the shear specific coefficients [N/mm^2], l_j is the length of cutting edge of the jth tooth [mm], A_{zj} is the cross sectional area of cut of the jth tooth [mm^2], φ_j, φ_{rj} are the instantaneous positioning angles of the jth cutting edge [rad], z_c is the active number of teeth.

In order to calculate the instantaneous cutting forces (F_y, F_z) it is necessary to determine cross sectional area of cut and active length of cutting edge, as well as calibrate specific coefficients. These parameters' values were estimated with the application of methods and data presented in Ref. [20], which was focused on the cutting forces modeling during ball end milling of hardened alloy steel.

The proposed model, described by Eq. (1) refers to the two different mechanisms of the milling tool's displacement. The first one can be observed mainly during machining with relatively large cross sectional areas of cut (and thus cutting forces – e.g. roughing, semi-roughing), or/and for the machining with the application of very slender tools (e.g. micromilling with tool diameters below 0.4 mm). In this case, the displacements are primarily caused by the tool's deflections, which are resulting from variable cutting forces. The cutter's displacements induced by the geometrical errors have in this case the lesser contribution. The above-mentioned mechanism will appear when the cutter's deflections are significantly higher than cutter's displacements resulting from the geometrical errors of the spindle–toolholder–milling tool system: $y_d \gg y_r$.

Fig. 4 depicts ball end mill's displacements, calculated on the basis of Eq. (1) and method presented in this chapter. This chart refers to the roughing milling, in which the following condition is fulfilled: $y_d \gg y_r$. It can be seen that amplitude of cutter's displacement is connected directly with the tooth passing frequency, which can be described by the following expression: $f_{zo} = z \cdot n/60$.

The second mechanism of the cutter's displacement can be observed during finishing processes or machining with the application of rigid tools (e.g. with the slenderness below 10 mm^{-1}). In this case, the displacements are primarily caused by the geometrical errors of the spindle–toolholder–milling tool system. The above-mentioned mechanism will appear

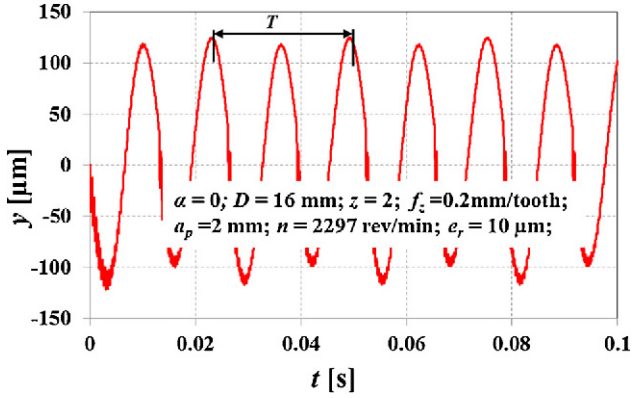

Fig. 4 – The modeled ball end mill's instantaneous displacements during roughing ($y_d \gg y_r$), number of teeth z = 2.

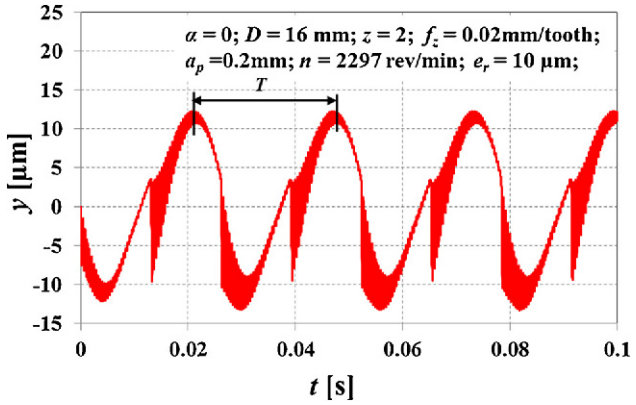

Fig. 5 – The modeled ball end mill's instantaneous displacements during finishing ($y_d \approx y_r$), number of teeth z = 2.

when the cutter's deflection values are comparable or even lower than the cutter's displacement values resulting from the geometrical errors: $y_d \leq y_r$. The modeled instantaneous displacements of the ball end mill during the finishing process are presented in Fig. 5. In this case the following condition was fulfilled: $y_d \approx y_r$.

Fig. 5 reveals that amplitude of cutter's displacement is connected directly with the rotational speed's frequency, which can be expressed by the following equation: $f_0 = n/60$.

3. Experimental details

3.1. Work and tool materials

Investigations have been carried out on hardened alloy steel 55NiCrMoV6 plate with hardness approx. 55 HRC. Monolithic ball end mill made of sintered tungsten carbide with diameter $D = 16$ mm and number of teeth $z = 2$ was selected as milling cutter. Tool made of fine-grained tungsten carbide had anti-wear TiAlN coating and the geometry: orthogonal rake angle – $\gamma_0 = -15^\circ$, helix angle – $\lambda_s = 30^\circ$, cutting edge radius – $r_n = 5$ μm, orthogonal flank angle – $\alpha_0 = 6^\circ$.

Table 1 – Cutting parameters applied in the research.

α [°]	f_z [mm/tooth]	a_p [mm]	v_c [m/min]	n [rev/min]
0; 30; 60	0.02; 0.16	0.2; 0.5	100	2297–8953

In order to solve differential motion equation (3), modal parameters (m, c, k) of the toolholder–milling tool system were selected from the previous work [21]: $m = 0.079$ N s^2/m, $c = 40.8$ N s/m, $k = 19492469$ N/m. The measurement was carried out on the joining part of the tool fixed in the thermal HSK toolholder. The tool's overhang was $l_n = 44$ mm.

3.2. Research range and method

The measured quantities in the carried out research were ball end mill's instantaneous displacements $y(t)$, cutting forces in machine tool coordinates (F_y, F_z) and static radial run out e_r. Milling tests were carried out in conditions of upward ramping with $\alpha > 0$ and slot milling with $\alpha = 0$. Cutting parameters applied in the research are presented in Table 1. Experiments were conducted on 5-axes CNC milling workstation (DMU 60monoBLOCK). In all investigated cases tool's effective diameter was lower than the value of pick feed.

The static radial run out was evaluated with the application of the incremental positioning sensor (Fig. 6). The run out's parameters e_r and δ were measured on the joining part of the tool. On the basis of carried out measurements the following values were obtained: $e_r = 10$ μm, $\delta = 0^\circ$.

The instantaneous cutter's displacements $y(t)$ were evaluated with the use of laser displacement sensor optoNCDT Micro-Epsilon, type 1700-10LL (Fig. 7). The laser's beam wavelength was $\lambda = 670$ nm, the measuring range was 10 mm and FSO (full-scale output) resolution at sampling frequency of 2500 Hz was equaled to 0.5 μm. The measurements were carried out on the joining part of the tool (at constant distance $l_m = 12$ mm from the collet), because it is

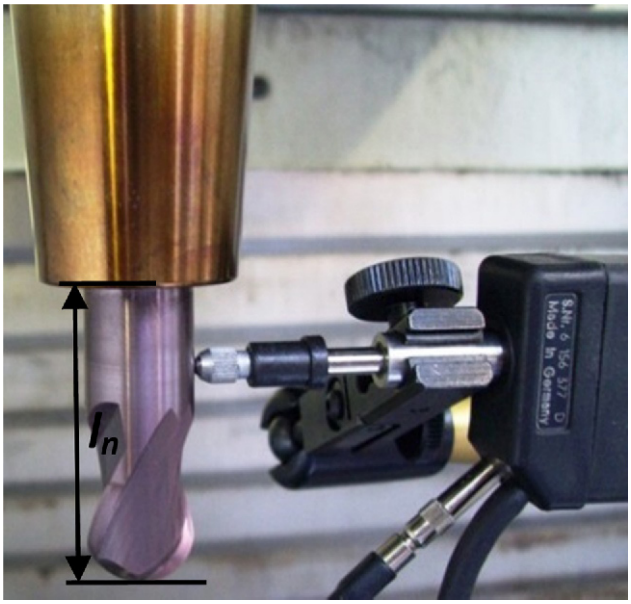

Fig. 6 – Radial run out's measurement setup.

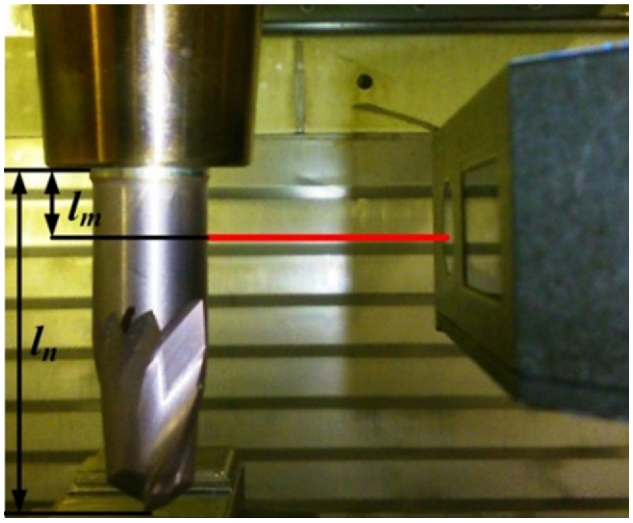

Fig. 7 – The scheme of ball end mill's displacement measurement with laser sensor.

impossible to conduct the measurement on the working part of tool during milling. The signals were acquired in time domain with the use of ANALIZATOR software.

The unfiltered signal of instantaneous tool's displacement acquired with the application of laser displacement sensor consists of many constituents connected directly with milling kinematics, as well as dynamical properties of the machine-toolholder-tool system. However the research was focused only on displacements generated by the milling kinematics and cutter's run out. Therefore, in order to eliminate the undesirable conditions influencing the acquired signals, the software low-pass Chebyshev's filter was applied. The cut off frequency f_c was determined on the basis of the following expression:

$$f_c \approx 2 \cdot f_{zo} + 10\% \tag{7}$$

Investigations were also focused on relations between the cutter's displacements and cutting forces induced during milling. In order to measure cutting force components, the piezoelectric force dynamometer was applied. Its natural frequencies are as follows: $f_{d\_X,Y} = 1672$ Hz, $f_{d\_Z} = 2280$ Hz. In order to avoid disturbances induced by proximity of forcing frequency to gauge natural frequency, the band-elimination filter was applied. Cutting force components were measured in machine tool's coordinates, in feed, and thrust directions, because of their effect on normal force generation, and thus cutter displacements y(t). The sampling frequency was $f_s \approx 20{,}000$ Hz.

3.3. *Results and discussion*

Fig. 8 depicts the modeled and measured ball end mill's displacement time courses $y = f(t)$, obtained for the various surface inclination angles α, cutting depths a_p and feeds f_z.

From the comparison of Fig. 8a and Fig. 8b it is resulting that the increase in depth of cut (from 0.2 mm to 0.5 mm) and feed per tooth (from 0.02 mm/tooth to 0.16 mm/tooth) has the direct effect on the displacement signal's amplitude and shape. This dependency is seen both for the modeled and measured signals. In case when, depth of cut $a_p = 0.2$ mm and feed $f_z = 0.02$ mm/tooth, the displacement amplitude is lower than that obtained for the ball end milling with $a_p = 0.5$ mm and $f_z = 0.16$ mm/tooth (Fig. 8b). The value of displacement's amplitude (Fig. 8a) is similar to the radial run out's value ($e_r = 10$ μm), whereas the signal's shape is similar to sine function with the period T equaled to the tool's revolution time. Furthermore, the signal presented in Fig. 8a is not affected by the appearance of peaks related to the immersion of the teeth into the work piece. On the other hand, during the milling with higher depth of cut and feed (Fig. 8b), the appearance of the displacement peaks related to the immersion of the cutter into the work piece is clearly seen.

This observation can be also confirmed by the spectrum analysis of the measured displacement signal, based on the Fast Fourier Transform (Fig. 9a and b). During the test with lower cutting conditions (Fig. 9a), the dominant peak has the frequency which corresponds to rotational speed f_o. However, for the milling with higher cutting conditions (Fig. 9b) the dominant peak's frequency is equaled to the tooth passing frequency f_{zo}. Nevertheless, this spectrum consists also of the harmonics of f_o and f_{zo} frequencies. The differences between the $y = f(t)$ charts, obtained for various cutting conditions (Fig. 8a and Fig. 8b) are caused by the different proportions between the tool's deflections y_d and displacements caused by run out y_r. In case with lower cutting parameters (and thus cross sectional area of cut A_z values), the cutting forces are low and consequently cause relatively small values of tool's deflections y_d.

According to the calculations based on Eq. (3), and Fig. 10a the maximal displacement y_{dmax} is 1.8 μm. This means that in this case: $y_r > y_d$, and cutter's displacements are mainly affected by the radial run out.

In case when cutting parameters are larger (Fig. 10b), the cutting forces and tool's deflections are higher ($y_{dmax} = 10.2$ μm). Thus, $y_r \approx y_d$, and cutter's displacements are affected both by the deflections and geometrical errors.

These observations are confirmed by the chart which presents maximal normal force values, obtained during milling with different cross sectional area of cut and surface inclination angle values (Fig. 11a). The $F_{n\ max}$ force values were determined on the basis of measured forces substituted into Eq. (4). Fig. 10a reveals that during milling with $a_p = 0.2$ mm and $f_z = 0.02$ mm/tooth ($A_{zmax} = 0.004$ mm^2) maximal normal force is significantly lower than that achieved for the cutting with the highest investigated cutting parameters ($a_p = 0.5$ mm, $f_z = 0.16$ mm/tooth, $A_{zmax} = 0.08$ mm^2). The differences between the force values are 5-fold in this case , which consequently influences the maximal cutter's displacements (see Fig. 11b).

It was also observed that surface inclination angle affects both measured and modeled tool's displacements (Figs. 8c, d and 11b). Nevertheless, this influence is connected mainly with the shape of the signal. During the slot milling with $\alpha = 0^\circ$ (Fig. 8c), the displacement signal is affected by the appearance of peaks related to the immersion of the cutter into the work material. However, the displacement signal acquired for the upward ramping $\alpha = 60^\circ$ (Fig. 8d) is similar to sine function with the period equaled to the tool's revolution time and amplitude

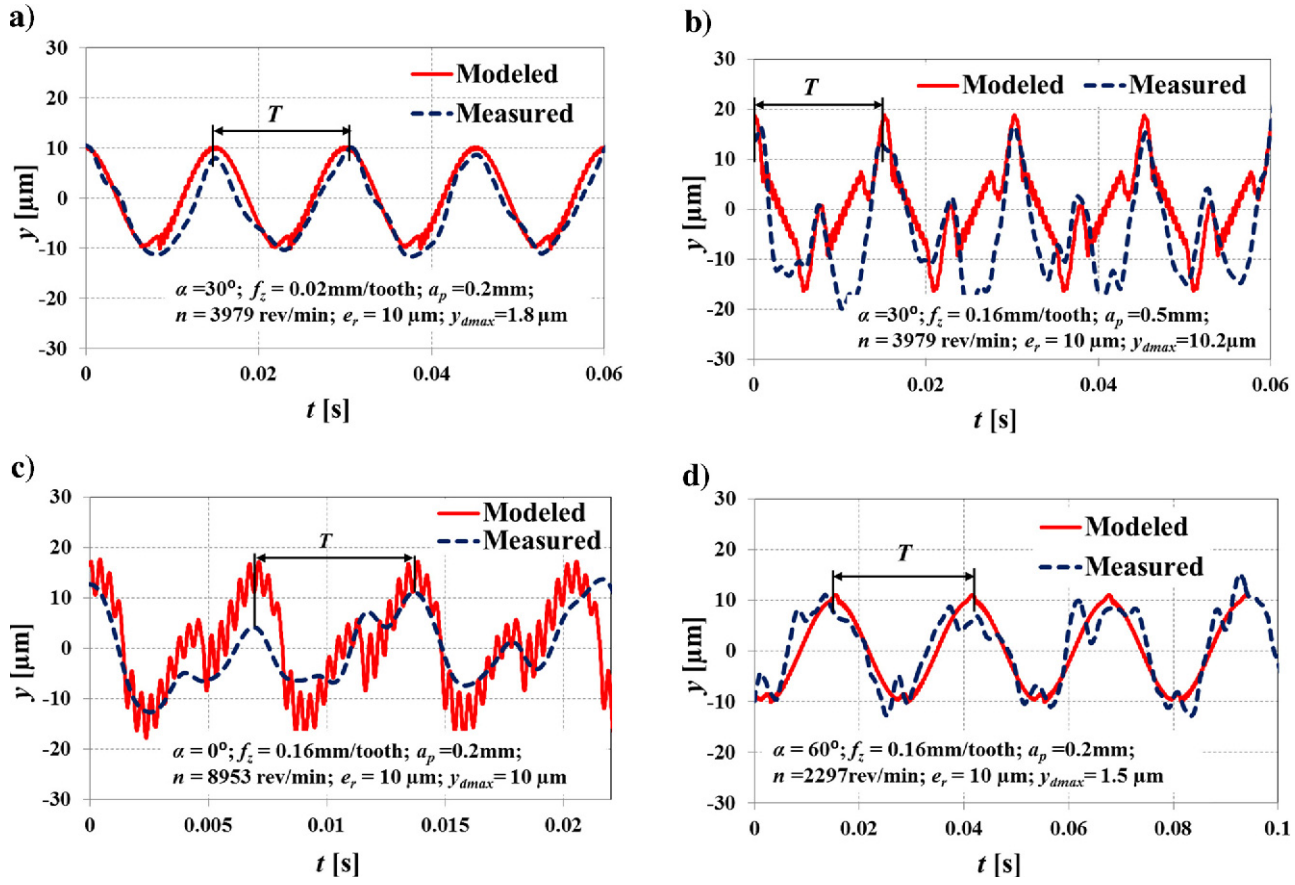

Fig. 8 – The modeled and measured signals of the ball end mill's displacement for: (a) $\alpha = 30^\circ$, $a_p = 0.2$ mm, $f_z = 0.02$ mm/tooth; (b) $\alpha = 30^\circ$, $a_p = 0.5$ mm, $f_z = 0.16$ mm/tooth; (c) $\alpha = 0^\circ$, $a_p = 0.2$ mm, $f_z = 0.16$ mm/tooth; (d) $\alpha = 60^\circ$, $a_p = 0.2$ mm, $f_z = 0.16$ mm/tooth.

equaled to radial run out's value. The diversified form of these signals can be attributed to the varied cutting force and tool's working angle values, obtained during the milling with various surface inclinations. According to the previous research [20], the highest cutting forces are observed for the milling with $\alpha = 0^\circ$, in comparison to the remaining modes with $\alpha > 0^\circ$. This tendency is also confirmed by Fig. 11a which shows that maximal value of normal force generated during slot milling is significantly higher than that achieved for the upward ramping with $\alpha = 60^\circ$. Consequently it affects cutter's deflections y_d and thus maximal displacements y_{max}, which values are higher during the slot milling, in comparison to those obtained for the upward ramping with $\alpha = 60^\circ$ (see Figs. 10c, d and 11b). Therefore, during the milling with $\alpha = 0^\circ$, cutter's displacements are affected both by the deflections and geometrical errors ($y_r \approx y_d$). However, during upward ramping

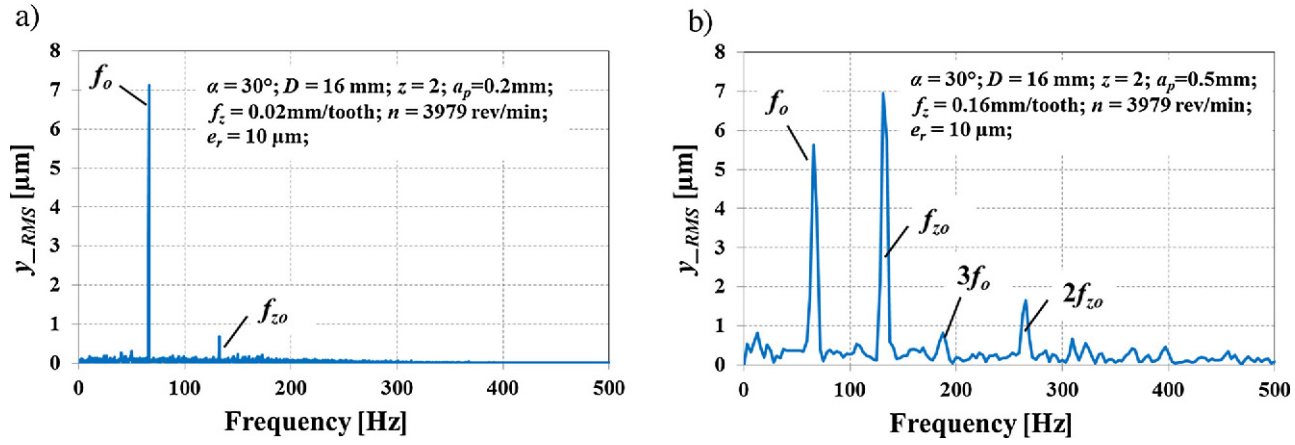

Fig. 9 – The FFT spectra of the measured displacement signal for: (a) $\alpha = 30^\circ$, $a_p = 0.2$ mm, $f_z = 0.02$ mm/tooth; (b) $\alpha = 30^\circ$, $a_p = 0.5$ mm, $f_z = 0.16$ mm/tooth.

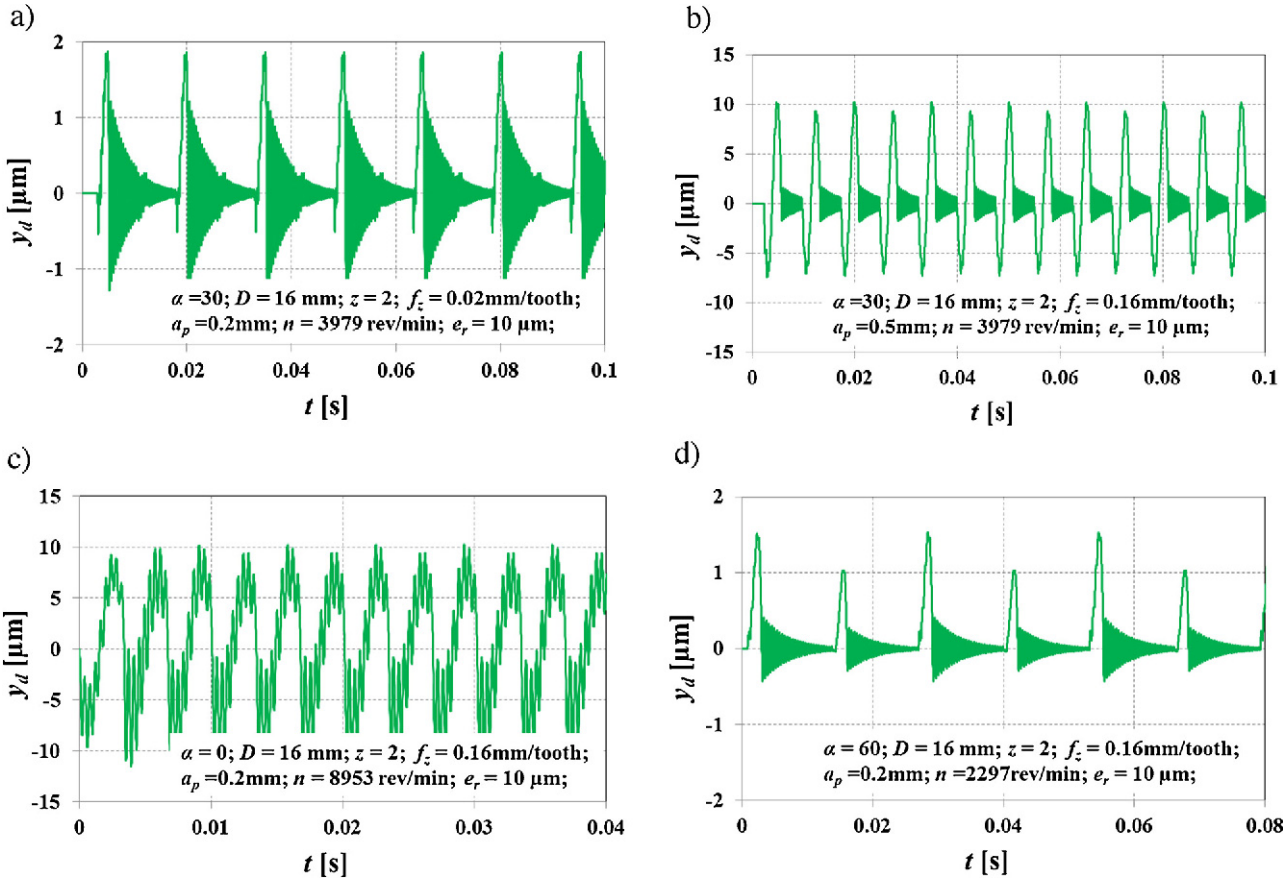

Fig. 10 – The modeled signals of the ball end mill's deflections for: (a) α = 30°, a_p = 0.2 mm, f_z = 0.02 mm/tooth; (b) α = 30°, a_p = 0.5 mm, f_z = 0.16 mm/tooth; (c) α = 0°, a_p = 0.2 mm, f_z = 0.16 mm/tooth; (d) α = 60°, a_p = 0.2 mm, f_z = 0.16 mm/tooth.

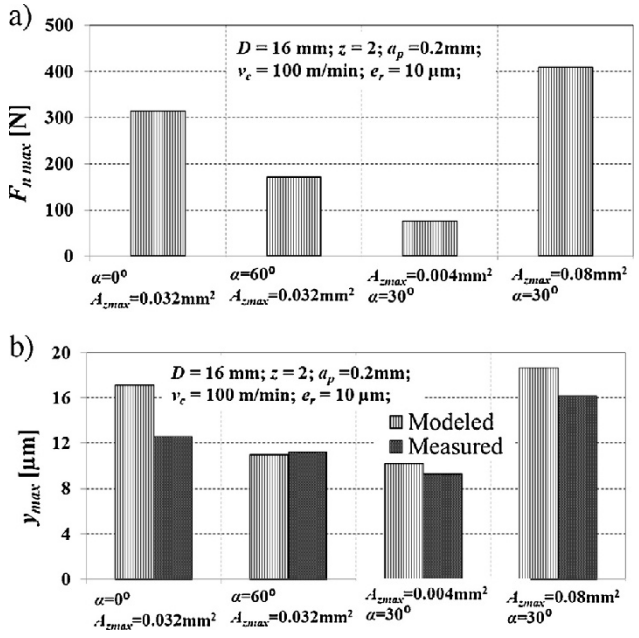

Fig. 11 – The influence of cutting parameters and surface inclination on: (a) maximal normal force values; (b) maximal cutter's displacement values.

with α = 60°, they are mainly affected by the geometrical errors induced by radial run out ($y_r > y_d$).

Research reveals that displacement signals estimated on the basis of the developed model stay in a good agreement with measured ones. Nevertheless some quantitative and qualitative discrepancies between these courses are found. Their appearance can be attributed to the cutting force model's accuracy (mainly specific force coefficients estimation), which influences cutter's deflections, or cutter's displacements measurement method (related mainly to the area of the displacement measurement, as well as filtration of the signal). These differences can be also caused by the modal parameters' identification which included only the properties of toolholder-milling tool system, without the consideration of machine tool's dynamical parameters. Therefore, the next researches should focus on the optimal selection of the displacement measurement parameters (e.g. the length of l_m section, cut off frequency) or on the accurate determination of modal parameters.

4. Conclusions

This work was concentrated on the modeling of cutter's displacements during ball end milling. The cutter's displacements model including: tool's geometry, cutting conditions,

surface inclination angle, run out and tool's deflections was proposed. The modeled instantaneous cutter's displacements were compared to those measured with the application of laser displacement sensor.

The simulations and measurements revealed that during ball end milling with axial depths of cut $a_p \le 0.5$ mm and feeds $f_z \le 0.16$ mm/tooth, tool's displacements are affected both by radial run out, and tool's deflections caused by cutting forces. It can be seen that the relations between the cutter's deflections and displacements induced by the geometrical errors are primarily described by the following expression: $y_d \le y_r$. This means that dynamical deflection model itself can be insufficient to the reliable estimation of ball end mill's working part displacement, especially during machining with the low sectional areas of cut and surface inclination angles: $\alpha > 0^\circ$. This observation can be attributed to the low slenderness ($l_n/D = 2.75$) of the applied tool, as well as to the relatively low cutting forces generated during finishing ball end milling.

It was proved that cutter's displacements are affected by cutting conditions (a_p, f_z), radial run out e_r and surface inclination angle α. Therefore, the high quality of the machined curvilinear surface can be achieved by the selection of the appropriate ball end milling tool's axis slope and minimization of the geometrical errors of the spindle–toolholder–milling tool system.

The proposed model can be further applied to the surface texture prognosis, during diversified milling operations and various tools' slenderness.

REFERENCES

[1] L.N. López de Lacalle, A. Lamikiz, J.A. Sanchez, M.A. Salgado, Toolpath selection based on the minimum deflection cutting forces in the programming of complex surfaces milling, International Journal of Machine Tools & Manufacture 47 (2007) 388–400.

[2] G.M. Kim, B.H. Kim, C.N. Chu, Estimation of cutter deflection and form error in ball-end milling processes, International Journal of Machine Tools and Manufacture 43 (9) (2003) 917–924.

[3] G.M. Krolczyk, S. Legutko, Experimental analysis by measurement of surface roughness variations in turning process of duplex stainless steel, Metrology and Measurement Systems 21 (4) (2014) 759–770.

[4] G.M. Krolczyk, P. Niesłony, S. Legutko, Determination of tool life and research wear during duplex stainless steel turning, Archives of Civil and Mechanical Engineering 15 (2) (2015) 347–354.

[5] P. Preś, W. Skoczyński, K. Jaśkiewicz, Research and modeling workpiece edge formation process during orthogonal cutting, Archives of Civil and Mechanical Engineering 14 (2014) 622–635.

[6] D. Przestacki, M. Jankowiak, Surface roughness analysis after laser assisted machining of hard to cut materials, Journal of Physics: Conference Series 483 (1) (2014).

[7] Y. Altintas, E. Budak, Analytical prediction of stability lobes in milling, CIRP Annals-Manufacturing Technology 44 (1) (1995) 357–362.

[8] E. Budak, Analytical models for high performance milling. Part I: Cutting forces, structural deformations and tolerance integrity, International Journal of Machine Tools & Manufacture 46 (2006) 1478–1488.

[9] L.N. López de Lacalle, A. Lamikiz, J.A. Sanchez, M.A. Salgado, Effects of tool deflection in the high-speed milling of inclined surface, International Journal of Advanced Manufacturing Technology 24 (2004) 621–631.

[10] T. Insperger, J. Gradisek, M. Kalveram, G. Stepan, K. Winert, E. Govekar, Machine tool chatter and surface location error in milling processes, Journal of Manufacturing Science and Engineering 128 (10) (2006) 913–920.

[11] P. Twardowski, S. Wojciechowski, M. Wieczorowski, T.G. Mathia, Selected aspects of high speed milling process dynamics affecting machined surface roughness of hardened steel, Scanning 33 (2011) 386–395.

[12] G. Peigne, H. Paris, D. Brissaud, A. Gouskov, Impact of the cutting dynamics of small radial immersion milling operations on machined surface roughness, International Journal of Machine Tools & Manufacture 44 (2004) 1133–1142.

[13] S. Seguy, G. Dessein, L. Arnaud, Surface roughness variation of thin wall milling, related to modal interactions, International Journal of Machine Tools & Manufacture 48 (2008) 261–274.

[14] M.H. Sadeghi, R. Salami, B.M. Imani, Dynamic force model for 3-axis ball-end milling of sculptured surfaces, in: Proceedings of Tehran International Congress on Manufacturing Engineering (TICME2005), December 12–15, Tehran, Iran, 2005.

[15] Y. Altintas, P. Lee, A general mechanics and dynamics model for helical end mills, CIRP Annals-Manufacturing Technology 45 (1) (1996) 59–64.

[16] Y. Sun, Q. Guo, Analytical modeling and simulation of the envelope surface in five-axis flank milling with cutter runout, Journal of Manufacturing Science and Engineering 134 (2012) 1–11.

[17] S. Wojciechowski, Machined surface roughness including cutter displacements in milling of hardened steel, Metrology and Measurement Systems 18 (3) (2011) 429–440.

[18] S. Wojciechowski, P. Twardowski, M. Pelic, Surface texture generation during cylindrical milling in the aspect of cutting force variations, Journal of Physics: Conference Series 483 (1) (2014).

[19] S. Wojciechowski, P. Twardowski, M. Wieczorowski, Surface texture analysis after ball end milling with various surface inclination of hardened steel, Metrology & Measurement Systems 21 (1) (2014) 145–156.

[20] S. Wojciechowski, The estimation of cutting forces and specific force coefficients during finishing ball end milling of inclined surfaces, International Journal of Machine Tools & Manufacture 89 (2015) 110–123.

[21] S. Wojciechowski, P. Twardowski, M. Pelic, Cutting forces and vibrations during ball end milling of inclined surfaces, Procedia CIRP 14 (2014) 113–118.